A LabVIEW-Based Implementation of Real-Time Underwater Acoustic OFDM System

Peng Chen[*], Yue Rong[*], Sven Nordholm[*], Alec J. Duncan[⋆], Zhiqiang He[†,♭]

[*]Department of Electrical and Computer Engineering, Curtin University, Bentley, WA 6102, Australia
[⋆]Department of Physics and Astronomy, Curtin University, Bentley, WA 6102, Australia
[†]Key Laboratory of Universal Wireless Communications, Ministry of Education,
Beijing University of Posts and Telecommunications (BUPT), Beijing, China
[♭]Key Laboratory of Underwater Acoustic Communication and Marine Information Technology, Ministry of Education,
Xiamen University, Xiamen, China

Abstract—The orthogonal frequency-division multiplexing (OFDM) technology receives increasing attention in underwater acoustic (UA) communications. This paper presents a real-time OFDM-based UA communication system, implemented using the National Instruments CompactDAQ device and the LabVIEW software. The system design including both the transmitter and receiver is discussed. The performance of this real-time system is verified through a UA communication experiment conducted recently in a tank. Compared with conventional digital signal processor (DSP)-based design, the proposed implementation simplifies the prototype design and reduces the software development time.

Index Terms—Underwater acoustic communication, OFDM, LabVIEW.

I. INTRODUCTION

The underwater acoustic (UA) channel, especially shallow water UA channel, is one of the most challenging channels for wireless communication, due to its extremely limited bandwidth, severe fading, strong multipath interference, and significant Doppler shifts [1]. Recently, orthogonal frequency-division multiplexing (OFDM) systems have been proposed for UA communication due to their strong capability in mitigating rapid frequency dispersion with reasonable computing complexity [2]-[9]. In [10], an implementation of OFDM-based modems for UA communication using the TMS320C6713 digital signal processor (DSP) development board has been demonstrated. However, such DSP-based implementation can be time-consuming on system design and development.

The National Instruments (NI) CompactDAQ device combined with the LabVIEW software provide an attractive solution to simplify the prototype design and reduce the software development time. NI CompactDAQ is a robust and reliable measurement system, capable of working with a series of NI input/output (I/O) modules. LabVIEW is a graphical programming language which simplifies hardware integration so that one can rapidly acquire and visualize data sets from NI or third-party I/O device virtually, resulting in a reduced programming and debugging time.
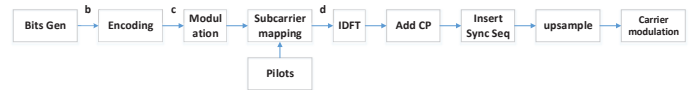
Fig. 1. Block diagram of the transmitter in a UA OFDM communication system.

In this paper, an NI LabVIEW-based implementation of real-time UA OFDM transceiver prototype is proposed. The system design including both the transmitter and receiver is discussed. The performance of this real-time system is verified through a UA communication experiment conducted recently in a tank.

The rest of this paper is organized as follows. The system model is introduced in Section II. The transmitter and receiver implementation is presented in Section III. The tank experiment results are demonstrated in Section IV. Conclusions and future works are discussed in Section V.

II. SYSTEM MODEL

In this paper, we use LabVIEW to implement a frame-based coded UA OFDM communication system. The block diagram of the transmitter is shown in Fig. 1. In each frame, a binary source data stream $\boldsymbol{b} = (b[1], \ldots, b[L_b])^T$ is generated, where $(\cdot)^T$ denotes the matrix (vector) transpose, L_b is the number of information-carrying bits in each frame. This binary stream is encoded by a turbo encoder, and then interleaved and punctured to form a coded sequence $\boldsymbol{c} = (c[1], \ldots, c[L_c])^T$ with length $L_c = R_m N_s N_b$, where R_m denotes the modulation order, N_s is the number of data subcarriers, and N_b denotes the number of OFDM blocks in one frame. The modulation module maps the coded sequence $\boldsymbol{c}$ into $N_s N_b$ data symbols taken from the phase-shift keying (PSK) constellations. Then every N_s data symbols together with N_p quadrature PSK (QPSK) modulated pilot symbols are mapped into one OFDM symbol vector $\boldsymbol{d} = (d[1], \ldots, d[N_c])^T$, where N_p and $N_c \geq N_p + N_s$ are the number of pilot subcarriers and total subcarriers, respectively. The pilot subcarriers are uniformly spaced.

Each OFDM symbol is converted to the time domain by the inverse discrete Fourier transform (DFT), leading to the following baseband discrete time signal

$$x = F^H d \tag{1}$$

where $(\cdot)^H$ denotes the conjugate transpose and F is an $N_c \times N_c$ DFT matrix with the (i, k)-th entry of $1/\sqrt{N_c}e^{-j2\pi(i-1)(k-1)/N_c}$, $i, k = 1, \dots, N_c$. A cyclic prefix (CP) longer than the channel delay spread is then prepended to x followed by upsampling and upshifting operations. Let f_{sc} and T_{cp} denote the subcarrier spacing and the length of CP, respectively. The bandwidth of the transmitted signal is $B = f_{sc}N_c$ and the duration of one OFDM symbol is $T = 1/f_{sc}$, while the total length of one OFDM block is $T_{total} = T + T_{cp}$.

At the receiver end, we assume a perfect synchronization. After downshifting, low-pass filtering, sampling the received signal at the rate of B and removing the CP, we obtain the baseband discrete time samples of one OFDM symbol as

$$\begin{aligned} r &= PF^H Dh_f + w \\ &= PF^H DFh_t + w \end{aligned} \tag{2}$$

where $D = \text{diag}(d)$ is a diagonal matrix taking d as the main diagonal elements, $r = (r[1], \dots, r[N_c])^T$, $w = (w[1], \dots, w[N_c])^T$ is the additive noise samples. In (2), $h_f = (h_f[1], \dots, h_f[N_c])^T$ is a vector containing the channel frequency response at all N_c subcarriers, $h_t = F^H h_f$ is the discrete time domain representation of the channel impulse response with a maximum delay of L_m, $P = \text{diag}(p)$, $p = (1, e^{-j2\pi f_o/B}, \dots, e^{-j2\pi(N_c-1)f_o/B})^T$ is the phase distortion caused by the Doppler shift, and f_o is the frequency offset.

After estimating and removing the frequency offset, the frequency domain representation of the received signal can be written as

$$\begin{aligned} r_f &= Fr \\ &= FF^H Dh_f + Fw \\ &= Dh_f + w_f \end{aligned} \tag{3}$$

where $w_f = Fw$ is the additive noise vector in the frequency domain.

III. System Implementation

A. System Hardware

An NI CompactDAQ system is adopted for signal generation and acquisition. It is a small modular data measurement and acquisition system capable of analog I/O, digital I/O, counter/timer operations, and industrial bus communication. It consists of a chassis and NI I/O modules.

1) NI cDAQ-9174: The cDAQ-9174 is a plug-and-play chassis designed for small portable sensor measurement systems. It controls the timing, synchronization, and data transfer among up to four I/O modules and an external host (e.g. desktop computer) via a USB cable. With this chassis, one is able to create a mix of analog I/O, digital I/O, and counter/timer
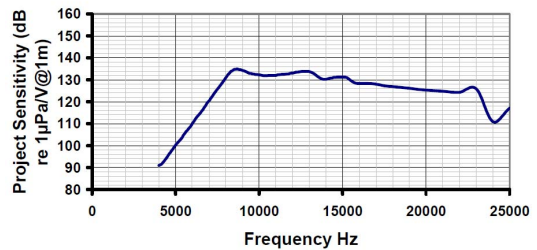

Fig. 2. Transmit sensitivity of CTG0052.

measurements. The cDAQ-9174 also has four 32-bit general-purpose counters/timers. With multiple timing engines, seven hardware-timed operations can be run simultaneously, with three independent rates for analog input.

2) NI-9232: The NI-9232 is a 3-channel dynamic signal acquisition module with a maximum sampling rate of 102.4k sample/s/ch. The input channels are able to measure signals simultaneously, and each channel has built-in anti-aliasing filters that automatically adjusts to its sample rate. The NI-9232 incorporates software-selectable AC/DC coupling. When used with NI software, this module provides processing functionality for condition monitoring such as frequency analysis and order tracking.

3) NI-9260: The NI-9260 is a 2-channel voltage output module. It features a 51.2k samples/s update rate, 24-bit resolution, 3 V output range, and ±30V over-voltage protection.

4) CTG0052 Transducer: The Chelsea Technologies CTG0052 acoustic transducer is a low frequency, high power projector-receiver transducer. The frequency range of the transducer is 8-16 kHz which covers the spectrum of telemetry, telephony or acoustic source needs in the underwater environment. The transmit sensitivity of CTG0052 is shown in Fig. 2.

5) HTI-96-Min hydrophone: The HTI-96-Min exportable hydrophone from High Tech Inc. is widely used in UA communications. The frequency range of this hydrophone is 2 Hz-30 kHz with a sensitivity of -201 dB re: 1V/μPa. One is able to connect this hydrophone with a voltage or current mode preamplifier.

B. Software Implementation

The software of our UA communication system is designed and implemented using NI LabVIEW which is an integrated graphical development environment. In the following, we present the software implementation at the transmitter and the receiver.

1) Transmitter: Key parameters of the system are summarized in Table I. The sampling rate is 48 kHz. Fig. 3 shows the frame structure of the transmitted signals. It can be seen that each frame contains $N_b = 5$ OFDM data blocks and one preamble block. The preamble block is a 64-pseudo noise (PN) sequence and is used for synchronization and frame head detection. Among the 512 subcarriers, there are 325 data subcarriers and 128 uniformly spaced pilot subcarriers. The data symbols are modulated by QPSK constellations encoded

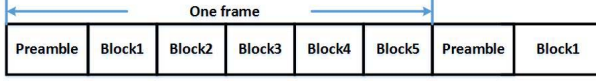| Bandwidth	B	4 kHz
Carrier frequency	f_c	12 kHz
Number of subcarriers	N_c	512
Subcarrier spacing	f_{sc}	7.8 Hz
Length of OFDM symbol	T	128 ms
Length of CP	T_{cp}	25 ms

Fig. 3. Frame structure of the transmitted signals.

by 1/3 rate turbo codes. As the number of information-carrying bits in each frame is $L_b = 1088$, the system source data rate is

$$R_b = \frac{L_b}{(T+T_{cp})N_b+64/B} = 1.39 \text{ kb/s.} \quad (4)$$

The flowchart of the data processing at the transmitter is shown in Fig. 4. After the system starts up, it first enters the idle mode and cleans the frame counter if required. Then the system checks the stop button (see Fig. 9) and stops running if required. Otherwise, the system checks the transmission button (see Fig. 9). If the system is not instructed to transmit a new frame, it remains in the idle state and starts the next checking run. Otherwise, the system enters the transmitting mode.

In the transmitting mode, the system firstly generates one data frame following the steps in Fig. 1. Then, the system increases the frame counter by one and forwards the generated data to NI-9260. At the end of the transmitting mode, the system enters the idle mode.

2) Receiver: The flowchart of the data processing at the receiver is illustrated in Fig. 5. After the system starts up, it enters the idle mode and cleans the counters if required. Then the system checks the status of the stop button (see Fig. 10) and stops running if required. Otherwise, the system checks the status of the receiving button (see Fig. 10). If the system is not instructed to receive signal, it remains in the idle state and starts the next checking round. Otherwise, the system enters the detection mode.

In the detection mode, the signal samples received from NI-9232 are converted first from the passband to the baseband.
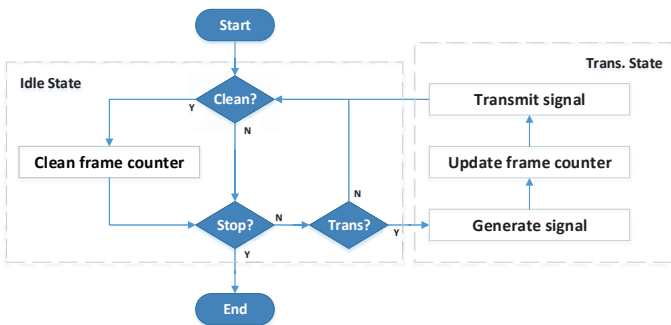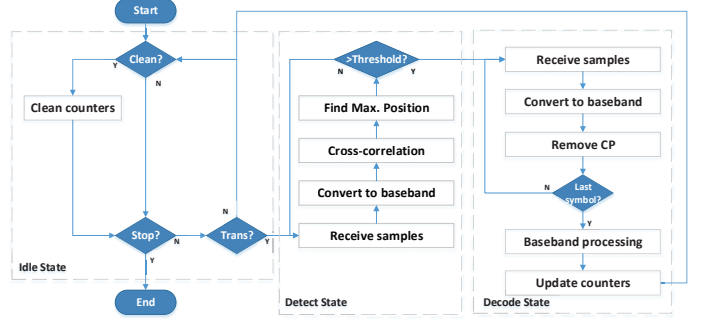

Fig. 4. Transmitter flowchart.
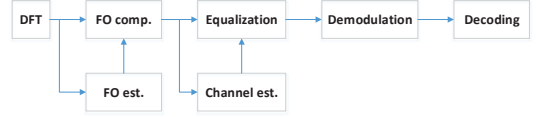

Fig. 5. Receiver flowchart.

Fig. 6. Block diagram of the baseband signal processing at the receiver.

Then the cross-correlation of the baseband received signal and the local synchronization sequence is performed. By checking the cross-correlation results, the receiver detects the received synchronization sequence which is the frame head.

After successful detection of the synchronization sequence, the receiver starts processing the data payload. The receiver first removes the CP from each OFDM block received by the NI-9232. The receiver then processes the received baseband signal which will be discussed later to obtain the decoded bits. The decoded bits are compared with the original bit sequence. Various counters, including the detected frame counter, the error bit counter and the successfully decoded frame counter, are updated. Finally the receiver enters the idle mode again.

The baseband signal processing at the receiver is shown in Fig. 6. It can be seen that the receiver performs frequency offset estimation and compensation for each OFDM symbol using the null subcarriers. Then the baseband signals are passed through channel estimation. The channel estimator uses the least-squares (LS) method to estimate the frequency domain channel response at the pilot subcarriers. Linear interpolation algorithm is then adopted by the estimator to estimate the data subcarrier channel response based on pilot subcarrier channel responses. The estimated channel response is used to equalize the received signals. Demodulation operation is performed to the equalized data subcarriers leading to a raw bit sequence. The raw bit sequence is finally passed through a turbo decoder. Note that in order to reduce the system computation time, the turbo encoder and decoder are implemented by the C Language and embedded into the system via the dynamic-link library (DLL) technology.

IV. EXPERIMENT RESULTS

In this section, we study the performance of our LabVIEW-based real-time UA OFDM system. The experimental system setup is shown in Fig. 7. In particular, the NI cDAQ-9174 is connected to a desktop computer through a USB cable
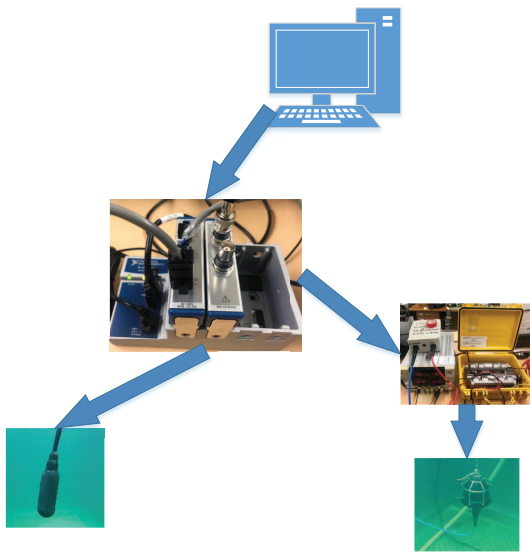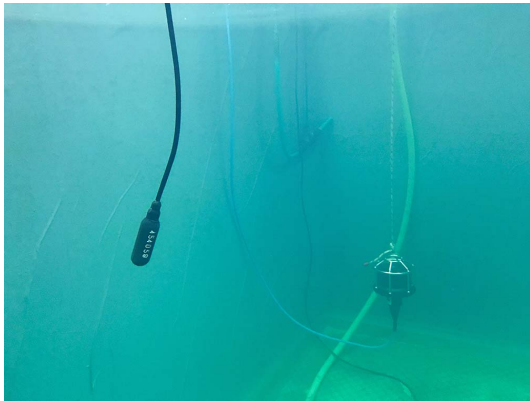
Fig. 7.   Experimental system setup.

Fig. 8.   Positions of the hydrophone and transducer in the tank.

Fig. 9.   Signal waveform and spectrum of one transmitted data frame.

Fig. 10.   A successfully detected data frame.

where the NI LabVIEW software is installed for the signal generation and processing. The NI-9232 and NI-9260 modules are plugged in slot 1 and slot 2 of the cDAQ-9174 chassis, respectively. The CTG0052 transducer with an amplifier is connected to channel 1 of NI-9260 for transmitting real-time acoustic signals. The channel 0 of NI-9232 is connected to the HTI-96-Min hydrophone for the acquisition of the real-time acoustic signals. Both the transducer and the hydrophone are placed in a tank whose length, width, and depth are 2.5 m, 1.5 m, and 1.8 m, respectively. Fig. 8 illustrates the positions of the transducer (right) and the hydrophone (left) in the tank. During the experiment, we bypassed the frequency offset estimation and compensation modules in Fig. 6 as the Doppler shift was very small in a tank.

Fig. 9 shows the signal waveform and spectrum of one transmitted data frame. Signal waveforms of a successfully detected data frame are shown in Fig. 10, including the passband signal, baseband signal with/without oversampling and the amplitudes of the cross-correlation result.

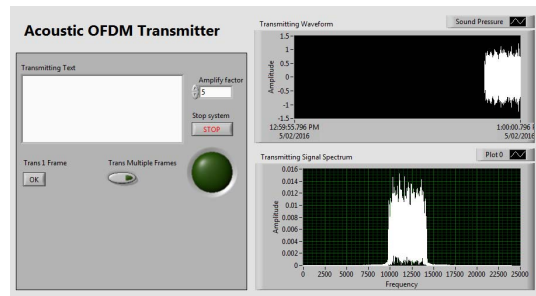Fig. 11 illustrates the first received OFDM symbol of a successfully decoded data frame, including the amplitude of the passband signal in the frequency domain, the amplitude of the baseband signal in the frequency domain, and the scatter plots of the received symbols before and after channel equalization. It can be seen that after the channel equalization, most of the QPSK symbols are properly aggregated into the normalized modulation constellations. It can also be observed from Fig. 11 that the received signal is interfered by low frequency noise. The reason for this phenomenon is under investigation.
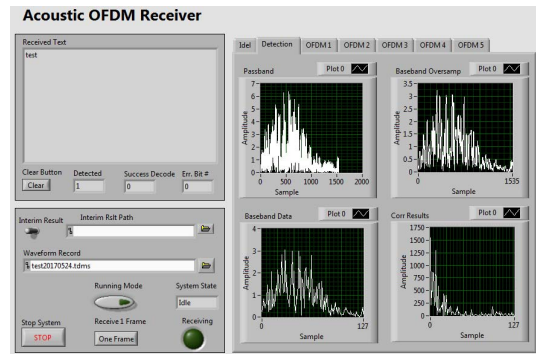
V. CONCLUSIONS AND FUTURE WORKS

In this paper, an NI LabVIEW-based implementation of real-time UA OFDM system has been presented. This system is divided into two sub-systems including the transmitter and the receiver. Both the transmitter and the receiver structures
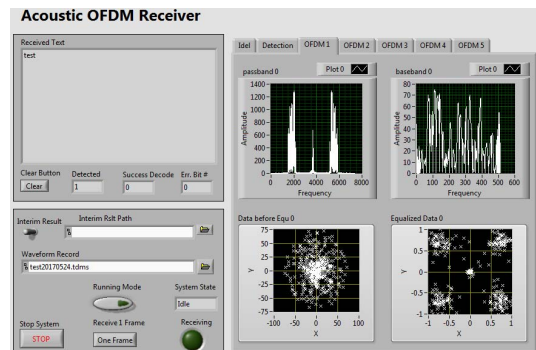

Fig. 11.   A received OFDM block.

have been illustrated. Tank test has been conducted to verify the performance of the system developed. In terms of future works, firstly, noise in the low frequency range observed from Fig. 11 needs to be mitigated. Secondly, the system is tested in an indoor tank with limited transmission range and Doppler shift. River and sea trials will be conducted in the near future to examine the system performance under more severe environmental conditions. Thirdly, we only adopt the LS-based channel estimator whose performance can be poor in some occasions. Advanced techniques will be considered to improve the channel estimation in the future.

REFERENCES

[1] D. Kilfoyle and A. Baggeroer, "The state of the art in underwater acoustic telemetry," *IEEE J. Ocean. Eng.*, vol. 25, no. 1, pp. 4-27, Jan. 2000.

[2] M. Chitre, S. H. Ong, and J. Potter, "Performance of coded OFDM in very shallow water channels and snapping shrimp noise," in *Proc. MTS/IEEE OCEANS*, Washington, DC, Sep. 2005, pp. 996–1001.

[3] B. Li, S. Zhou, M. Stojanovic, and L. Freitag, "Pilot-tone based ZP-OFDM demodulation for an underwater acoustic channel," in *Proc. MTS/IEEE OCEANS*, Boston, MA, Sep. 2006.

[4] B. Li, S. Zhou, M. Stojanovic, L. Freitag, and P. Willett, "Multicarrier communication over underwater acoustic channels with nonuniform Doppler shifts," *IEEE J. Ocean. Eng.*, vol. 33, no. 2, pp. 198-209, Apr. 2008.

[5] L. Wan, Z. Wang, S. Zhou, T. C. Yang, and Z. Shi, "Performance comparison of Doppler scale estimation methods for underwater acoustic OFDM," *Journal of Electrical and Computer Engineering*, vol. 2012, Artical ID 703243, 11 pages.

[6] Z. Wang, S. Zhou, J. Catipovic, and P. Willett, "Asynchronous multiuser reception for OFDM in underwater acoustic communications," *IEEE Trans. Wireless Commun.*, vol. 12, no. 3, pp. 1050-1061, Mar. 2013.

[7] P. Chen, Y. Rong, and S. Nordholm, "Pilot-subcarrier based impulsive noise mitigation for underwater acoustic OFDM systems," in *Proc. WUWNet 2016*, Shanghai, China, Oct. 24-26, 2016.

[8] P. Chen, Y. Rong, S. Nordholm, Z. He, and A. Duncan, "Joint channel estimation and impulsive noise mitigation in underwater acoustic OFDM communication systems," *IEEE Trans. Wireless Commun.*, vol. 16, no. 9, pp. 6165-6178, Sep. 2017.

[9] P. Chen, Y. Rong, S. Nordholm, and Z. He, "Joint channel and impulsive noise estimation in underwater acoustic OFDM systems," *IEEE Trans. Veh. Technol.*, to appear, 2017 (DOI: 10.1109/TVT.2017.2743220).

[10] H. Yan, L. Wan, S. Zhou, Z. Shi, J. H. Cui, J. Huang, and H. Zhou, "DSP based receiver implementation for OFDM acoustic modems," *Phys. Commun.*, vol. 5, no. 1, pp. 22-32, 2012.